Acta Scientiarum
http://periodicos.uem.br/ojs/acta
ISSN on-line: 1807-8664
Doi: 10.4025/actascitechnol.v42i1.45899

Removal of sodium compounds from Co/SBA-15 catalysts for Fischer-Tropsch Synthesis

Lidiane Sabino da Silva[1*], Gabriela Gonzaga Cher[1], Maria Auxiliadora Scaramelo Baldanza[2], Victor Luis dos Santos Teixeira da Silva[2] and Pedro Augusto Arroyo[1]

[1]Programa de Engenharia Química, Universidade Estadual de Maringá, Av. Colombo, 5790, 87020-900, Maringá, Paraná, Brazil. [2]Programa de Engenharia Química, Universidade Federal do Rio de Janeiro, Rio de Janeiro, Rio de Janeiro, Brazil. *Author for correspondence. E-mail: lidiane_eq@hotmail.com

ABSTRACT. In the present work, the synthesis of Co/SBA-15 catalysts intended for Fischer-Tropsch (FT) synthesis was performed. During the synthesis of catalysts there was contamination of samples with sodium nitrate due to the nature of the reducing agent used for the synthesis of metallic phase. This kind of impurity is not advantageous for the FT reaction. Attempts at removal of sodium compounds were carried out by means of simple leaching treatments, using ethanol and acid ethylenediaminetetraacetic (EDTA) as solvent and complexing agent, respectively, followed by heat treatment at temperatures of 150 or 300°C. It was possible to conclude that the treatment using EDTA was more effective in removing almost all the alkaline phase of samples, despite the occurrence of oxidation, agglomeration, and removal of the metal nanoparticles in this process. In addition, there were no significant differences in the product selectivity of FT synthesis of the catalysts after sodium removal, although the nanoparticles were larger than 10 nm.

Keywords: sodium removal; Fischer-Tropsch Synthesis; cobalt catalysts; EDTA; ethanol.

Received on December 19, 2018.
Accepted on July 17, 2019

Introduction

The Fischer-Tropsch process is an effective technology for converting carbon sources, such as coal, natural gas, and biomass, into high-value aggregated and pollutant-free products (Dry, 1996). Thus, since Brazil has abundant reserves of natural gas, Fischer–Tropsch synthesis (FTS) is highlighted as one of the main steps in the GTL (gas to liquid) process, which turns natural gas into liquid hydrocarbons (Ramos et al., 2011).

The aforementioned catalytic reaction converts two of the simplest compounds of nature, H_2 and CO (synthesis gas), into a complex array of products, including olefins, alkanes, and oxygenated compounds, in addition to water, according to Dalai and Davis (2008). The main objective is to produce hydrocarbons in the range of fuels such as diesel, kerosene, and gasoline.

Although several metals are active in FTS, only iron and cobalt are economically viable for use as active metal on an industrial scale (O'Brien et al., 1997). Cobalt-based catalysts have been widely studied in FTS due to their high activity, high resistance to deactivation, and low activity in the shift reaction (Martínez, López, Márquez, & Díaz, 2003). In addition, cobalt is the most indicated metal when the synthesis gas is obtained from natural gas, due to the high H_2/CO ratio (Davis, 2003).

In order to achieve a larger number of active sites, supported catalysts are commonly used because they allow the dispersion of the metallic phase over a high specific area. Due to its narrow size distribution, high specific area, and high thermal stability in relation to other mesoporous materials (Zhao, Sun, Li, & Stucky, 2000), SBA-15 is a good alternative for use as catalyst support.

Alkali and alkaline metals earths may be accidentally inserted into the catalysts intended for FTS during the preparation steps. These components may be introduced, for example, by impurities present in the water, precursors of promoters and active metals, and equipment used in the process, as well as by the synthesis gas derived from biomass (An et al., 2007; Lillebø, Patanou, Yang, Blekkan, & Holmen, 2013). Several studies show a decrease in the activity of catalysts and increase in the selectivity of CO_2 as the amount of sodium increases in the samples (An et al., 2007; Borg et al., 2011; Balonek et al., 2010; Lillebø et al., 2013). These behaviours are to a lesser extent attributed to geometric effects of the alkaline surface

and to a greater extent to electronic effects, which can affect the adsorption and desorption of H_2 and CO molecules (Balonek et al., 2010), leading to the need to remove alkaline compounds present in catalysts.

Currently, there are almost no studies on procedures for removal of alkali compounds in catalysts, for this reason this work presents a leaching procedure was carried out with the aim of removing sodium compounds present in the Co/SBA-15 catalysts. The solvents used were ethanol and ethylenediaminetetraacetic acid (EDTA). The former was chosen because it is a good solvent for sodium nitrate, and the second, being a polydentate binder, can forms complexes with various metal ions. The alkaline phase was inserted unintentionally by the use of sodium borohydride as a reducing agent in the synthesis of the active phase. The method promotes the removal of sodium compounds through a simple and fast procedure, allowing the use of catalysts without the presence of poisoning compounds in the FTS.

Material and methods

Experimental

Catalysts

The mesoporous molecular sieve SBA-15 used as catalyst support was synthesized according to the procedure presented by Zhao et al. (1998; 2000). The synthesis of cobalt nanoparticles was performed according to the method proposed by Zhao, Zheng, Zhang, and Xiao (2003).

Cobalt nanoparticles having a size of approximately 5 nm were incorporated in the mesoporous supports by incipient impregnation. The suspension of nanoparticles was slowly dripped on the support to obtain a content of around 7% by mass of cobalt. Subsequently, the sample was kept in a desiccator at room temperature under vacuum for drying.

Leaching

The leaching procedure was carried out in catalysts in order to remove the sodium compounds present. The treatments consisted of a washing step and a heat treatment stage. The samples were washed with 99.5% ethanol or EDTA (0.3 mol L^{-1}) in catalyst/ethanol volumetric proportions of approximately 1:3 and then centrifuged for 10 min. at 3500 rpm. After centrifugation, the samples were dried in a desiccator at room temperature under vacuum for seven days. Subsequently, catalysts were subjected to heat treatment for a period of 3 hours at temperatures of 150 or 300°C. Table 1 shows the nomenclature and conditions used in the treatment of each sample.

Characterizations

The X-ray diffraction (XRD) patterns were collected with a Shimadzu XRD6000 X-ray diffractometer using Ni-filtered Cu-Kα (40 kV and 30 mA) radiation with a diffraction angle (2Θ) ranging from 5 to 60º. The peaks were identified by means of the computational package PCPDFWIN v. 2.3.

The catalysts were analysed by Transmission Electron Microscopy (TEM) and High-Resolution Transmission Electron Microscopy (HRTEM) using a JEM 1400 and a JEM 3010 URP, respectively. The samples were prepared using a small amount of nanoparticles suspension in isopropyl alcohol. After the preparation, the suspension was kept for about an hour in an ultrasound bath with the aim of achieving maximum Co/SBA-15 dispersion in the medium. Then, a drop of solution was placed carefully on a laced (or holey) carbon-coated copper grid (0.3 cm in diameter and 200 mesh from Ted Pella, Inc.), which was subsequently dried at room temperature. The grids prepared for analysis were dried overnight at room temperature and subsequently inserted into a microscope to obtain the images.

Table 1. Nomenclature and conditions used in leaching treatment.

Sample	Solvent	Number of washes	Heat treatment (°C)
Standard	–	–	–
Et/1/150	Ethanol	1	150
Et/1/300	Ethanol	1	300
Et/5/150	Ethanol	5	150
Et/5/300	Ethanol	5	300
Ed/5/150	EDTA	5	150
Ed/5/300	EDTA	5	300

Analyses of nitrogen adsorption/desorption were carried out at −196°C on a Micromeritics ASAP 2020 apparatus using approximately 0.100 g of sample for each measurement. Before the measurements, the samples were degassed under vacuum condition at 300°C for 3 hours. The specific surface areas were evaluated using the Brunauer–Emmett–Teller (BET) method in the P/P_0 range of 0.05–0.3 (Brunauer, Emmett, & Teller, 1938). The mesopore diameter was calculated from the desorption branch of the nitrogen isotherms using the Barrett–Joyner–Halenda (BJH) method (Barrett, Joyner, & Halenda, 1951), calibrated for cylindrical pores (Kruk & Jaroniec, 1997). The total pore volumes were estimated according to nitrogen uptake at a relative pressure (P/P_0) of 0.99.

The cobalt contents present in the catalysts were determined by atomic absorption (AA) in Varian 50B equipment. Prior to analysis, the samples were digested as follows: approximately 0.2 g of the sample was mixed with 0.5 ml of aqua regia (HNO_3: HCl at 1:3) and 3.0 ml of hydrofluoric acid; then the solution was heated until it became clear. The solutions were cooled and then 10 mL of water, 5.0 mL of 4% H_3BO_3, and 1.0 mL of hydrochloric acid were added. After further heating, the solutions were cooled, transferred, and diluted in 100 mL volumetric flasks. The solutions were then immediately stored in plastic bags prior to analysis to avoid the risk of contamination. Solutions with concentrations of 40, 80, 120, and 200 mg L^{-1} of Co were used to prepare the calibration curve, obtained from a standard solution of cobalt.

The identification of compounds present on the surface of the SBA-15 was performed by spectroscopy analysis in the Fourier transform infrared (FTIR) region using a Bruker Vertex 70 V spectrophotometer. The preparation of KBr tablets was necessary for the analysis. Thus, 199 mg of KBr was mixed with 1 mg of each sample until the blend became homogeneous, and then the powder was pressurized to form pellets of a size and thickness suitable for use in the equipment.

Fischer-Tropsch Synthesis (FTS)

The catalytic tests were carried out on a bench unit composed of an Inconel reactor, a thermostatic bath, two resistive furnaces, temperature controllers, thermocouple to monitor reactor temperature, lines, valves, a line-coupled chromatograph, and a computer for data acquisition and analysis.

Before the reaction, all the catalysts were activated with pure hydrogen (50 mL $min.^{-1}$) and a heating rate of 5 °C $min.^{-1}$ until a temperature of 365°C was reached for 10 hours. After the reduction, the system was cooled to 210°C under H_2 atmosphere. The sample was then purged under inert atmosphere (He, 50 mL $min.^{-1}$) for 30 min.

The reaction conditions used in the catalytic evaluation were as follows: Temperature, 210°C; Pressure, 20 atm; H_2/CO Ratio, 2.0; Flow of CO/H_2/N_2, 30 mL min^{-1} (N_2 is used as internal standard).

The reaction products were analysed in a gas chromatograph coupled in line with FID and BID flame ionization detectors. The CO conversion was calculated by means of continuous measurements using an He plasma detector and N_2 as an internal standard. The monitoring of product formation was carried out by analyses in a flame ionization detector. An internal standard was used to obtain the amount of liquid and gaseous hydrocarbons produced during the reaction. Finally, mass selectivity was calculated from the following Equation 1 at 3:

$$Area_i\% = \frac{Area_i}{Area_{total}} \times 100 \quad (1)$$

$$Flowrate_i = \frac{Area_i\%}{100} \times HC_{flowrate}^{gas} \quad (2)$$

$$Selectivity_i = \frac{flowrate_i}{totalHC_{flowrate}} \times 100 \quad (3)$$

where:

$Area_i$ and $Area_{total}$ refer to the areas obtained in chromatograms.

Results and discussion

The results corresponding to XRD analysis of catalysts are shown in Figure 1. In some catalysts, peaks are observed at 2θ = 29.5□ and 2θ = 39□, which are indexed to the planes (104) and (113), respectively, indicating the presence of sodium nitrate (PCPDFWIN 89-0311), which is a secondary product in the

reduction reaction of cobalt nitrate with sodium borohydride. As previously explained, the presence of these compounds is not interesting for the FTS.

There was a significant positive removal of sodium compounds after washing and heat treatment. By washing the catalysts with ethanol only once, the amount of sodium nitrate removed increased after heat treatment at a higher temperature. This suggests that part of the alkaline compounds, which were not removed with the solvent after centrifugation, was removed during the heat treatment. By washing the catalysts five times with ethanol or EDTA followed by subsequent heat treatment, there is apparently no presence of the undesired phase.

However, the alkaline phase could still be present in the catalysts if the particles were less than 5 nm in size. This behaviour occurs because the XRD technique is not sensitive to the presence of very small oxide crystals; in this case, the peaks become too wide and insufficiently intense to be identified and measured (Khodakov, Chu, & Fongarland, 2007). For this reason, FTIR was subsequently performed with the objective of verifying whether sodium was still present in the samples.

HRTEM was performed on the catalysts prior to leaching to observe the distribution, state, and size of the nanoparticles in the mesoporous support. Some images obtained are shown in Figure 2.

According to Figure 2, there is a good agreement between the impregnated particle sizes and those visualized on the catalysts. Interplanar distances of approximately 0.205 nm were found, which were equivalent to the crystalline plane (111) of the metallic cobalt fcc (Co^0) (Martínez, Prieto, & Rollan, 2009). It was not possible to obtain measures related to the interplanar distances of the oxide species, probably due to its absence in significant quantity, since the catalysts presented a greyish colouration, indicating the presence of cobalt metallic.

TEM analyses were carried out in some samples after leaching and are shown in Figure 3. According to Figure 3a and b, the heat treatment contributes in part with the agglomeration of the metal nanoparticles, which showed sizes of around 20 nm, confirming the occurrence of sintering.

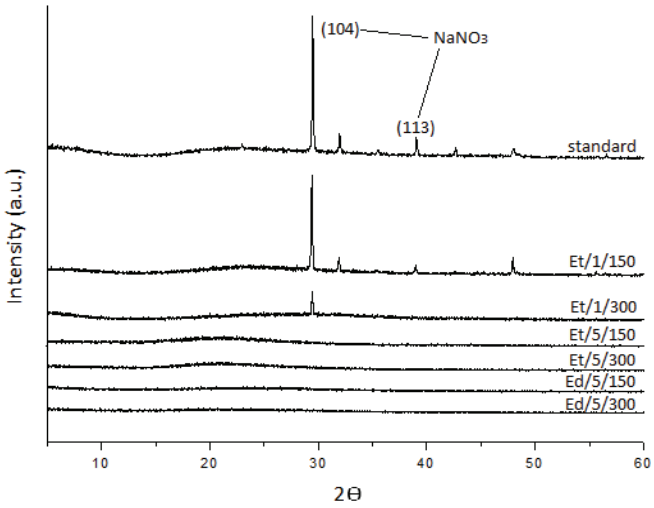

Figure 1. X-ray diffraction of catalysts before and after leaching treatments.

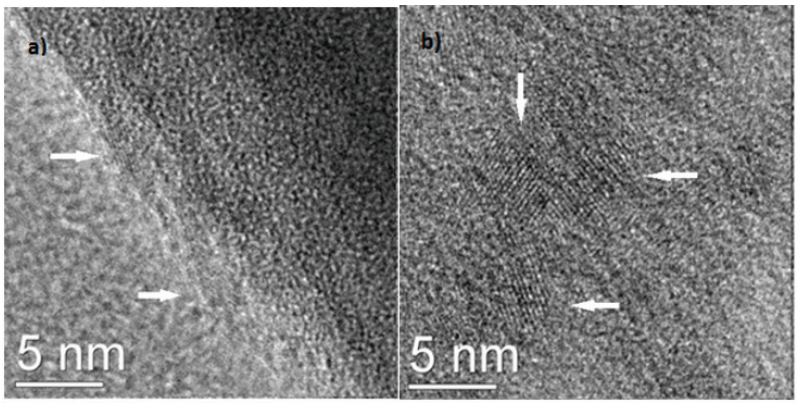

Figure 2. HRTEM images of the catalysts prior to leaching.

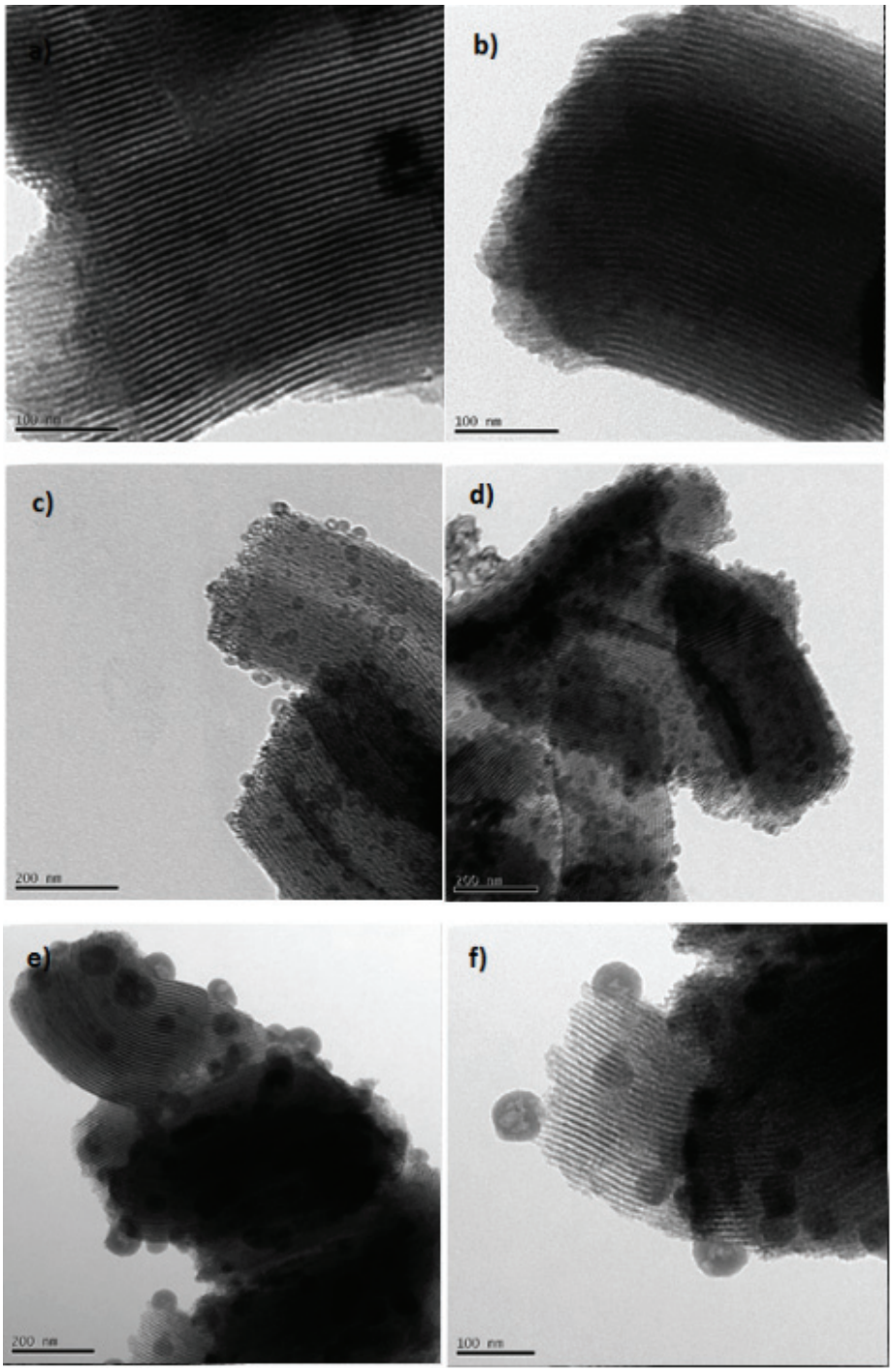

Figure 3. TEM images of the catalysts after leaching; a and b) catalysts before leaching and treated at 300°C for 3 hours; c and d) Et/5/300; e and f) Ed/5/300.

Moreover, after the washing steps there was a larger agglomeration, as can be seen in Figure 3c-f, which showed particle sizes in the range of approximately 20 to 50 nm. This proves the potential for agglomeration of the nanoparticles by using ethanol and EDTA as solvents during leaching. However, these findings contrast with previous results reported in the literature (Loosdrecht, Haar, Kraan, Dillen, & Geus, 1997; Mochizuki, Hara, Koizumi, & Yamada, 2007), which state that the use of chelating agents in the catalysts promotes a greater dispersion and, consequently, a decrease in the nanoparticle size.

This apparent lack of correlation can be attributed to the centrifugation step, which may have caused the agglomeration of the nanoparticles, since the non-leached samples showed less agglomeration. This result is extremely important considering that the FTS occurs in the same temperature range of the heat treatment and that the particle size significantly influences the activity and selectivity of the catalyst (Wang, Wu, Zhang, & Tang, 2005; Bezemer et al., 2006; Borg et al., 2008).

The N_2 adsorption/desorption isotherms of the Co/SBA-15 catalysts are shown in Figure 4. All the isotherms presented are of type IV and have H1 type hysteresis, thus showing that the samples maintained the characteristics of the mesoporous material even after the stages of washing and heat treatment.

Table 2 presents the textural parameters of the synthesized catalysts. There was a decrease in the volume of N_2 adsorbed on the catalysts treated with ethanol. This fact suggests the agglomeration of cobalt species in the channels or in the pore mouth on the external surface, partially blocking their entry and thus hindering the access of nitrogen to its interior.

However, in the catalysts treated with EDTA, there is an increase in the values of the textural parameters after washing and heat treatment. This may be due to the fact that the formation constant of Co-EDTA complexes is greater than the Na-EDTA formation constant (Schwarzenbach & Flaschka, 1969). Thus, during the treatment with EDTA, besides the removal of sodium, the removal of part of the impregnated cobalt would also be occurring due to the formation of Co-EDTA complexes. This behaviour would lead to the non-obstruction of the catalyst pores and consequently to an increase in the parameter values like the specific area, volume, and pore size.

Through the atomic absorption analysis presented in Table 3, it is possible to confirm the formation of Co-EDTA complexes during the treatment, since in the Et/5/150 and Et/5/300 catalysts most of the impregnated cobalt is removed after treatment with EDTA. In the opposite way, Et/5/150 and Et/5/300 catalysts showed an increase in the cobalt concentration probably due to the removal of soluble substances in the medium, in addition to the sodium nitrate, which may be present in the catalyst.

Figure 5 presents the results related to the FTIR analysis. Characteristic bands of sodium nitrate, which is located at 1366 cm^{-1} according to the literature (Tam, Gunter, Craciun, Miller, & Jackson, 1997), are visualized in the spectra. After the treatments using ethanol, there sodium is still present in the catalysts, while the treatment using EDTA was more effective in removing the compounds. In this case, the heat treatment at a higher temperature allowed the removal, apparently almost complete, of sodium nitrate.

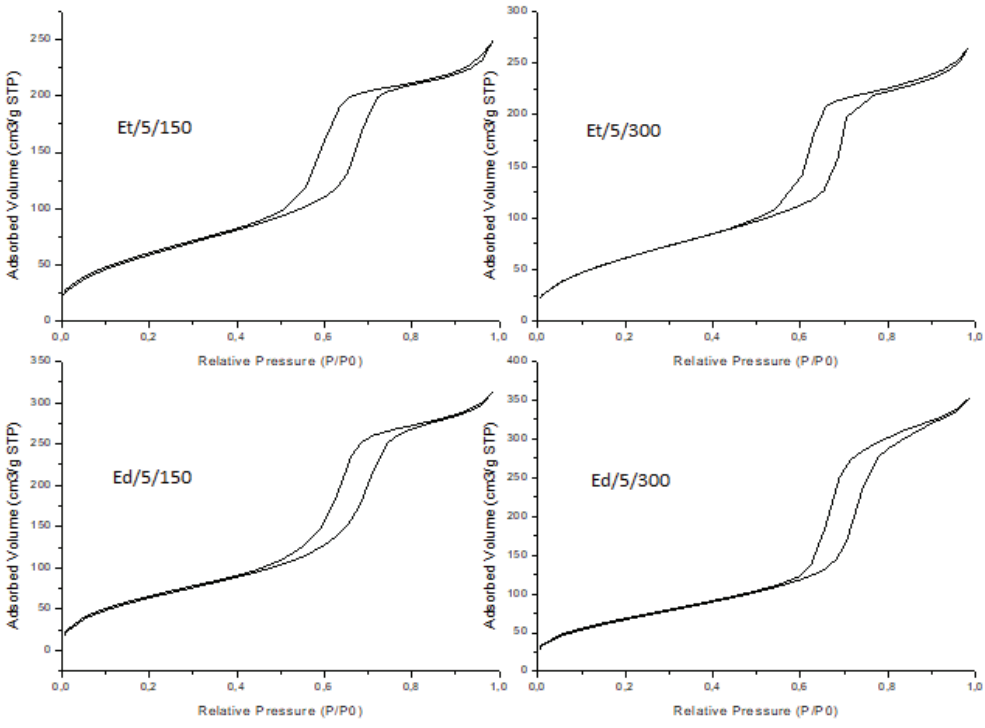

Figure 4. N_2 adsorption and desorption isotherms for Co/SBA-15 catalysts.

Table 2. Textural parameters of Co/SBA-15 catalysts.

Catalyst	Specific area (BET) $m^2\ g^{-1}$	V_{pores} ($cm^3\ g^{-1}$)	D_{pores} (Å)
Standard	247	0.458	58.8
Et/5/150	227	0.384	54.2
Et/5/300	240	0.410	55.6
Ed/5/150	251	0.484	57.8
Ed/5/300	250	0.545	70.3

Table 3. Cobalt content in catalysts.

Catalyst	Nominal content (%)
Standard	7.00
Et/5/150	7.15
Et/5/300	8.38
Ed/5/150	2.56
Ed/5/300	1.48

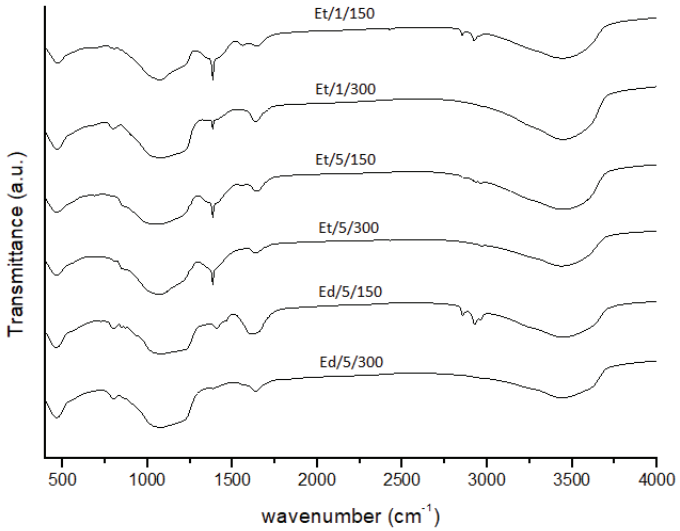

Figure 5. FTIR spectra of the CoSBA-15 catalysts.

Interestingly, the complexing power of EDTA was more effective than the dissolving power of ethanol in practically complete removal of the sodium compounds after heat treatment at the proper temperature. Without the presence of a significant amount of alkaline phase, the catalyst can achieve a better performance in specific processes, for example, in the FTS.

In Figure 6, Co/SBA-15 catalysts are shown after leaching and heat treatment. Cobalt nanoparticles in the metallic state are known to have black colouration (Sun & Murray, 1999). When these nanoparticles are impregnated in a white coloured support, such as the SBA-15, the sample will acquire greyish tones depending on the impregnated metal content. However, if the nanoparticles oxidize, the colouration can acquire pink, bluish, or similar tones, depending on the valence number of the metal. The different colours are related to the absorption of radiation in specific zones of the visible spectrum due to electronic transitions in the orbital d.

Although sodium compounds were removed after EDTA treatment, nanoparticles were oxidized, while treatment using ethanol kept the cobalt nanoparticles in the metallic state but left traces of sodium in the catalysts. Therefore, EDTA-treated catalysts require a reduction step prior to the catalytic evaluation in the FTS, requiring additional process costs, whereas in catalysts treated with ethanol this step could be omitted.

Through the catalytic evaluation of the samples Et/5/150, Et/5/300, Ed/5/150, and Ed/5/300, the behaviour of the catalysts was verified in the FTS. The product formation profile and CO conversion after 0.1 and 24 hours of reaction are shown in Table 4.

There were no significant differences in CO conversions of catalysts both at the beginning of the reaction and after the 24 hours interval. There was almost no difference in selectivity among the catalysts analysed, probably due to the fact that the nanoparticles presented a too large size after the treatments carried out with the objective of removing the sodium compounds. As previously mentioned, the catalysts evaluated presented nanoparticle sizes between 20 and 50 nm, and the ideal size seems to be below 10 nm, as reported in the literature (Bezemer et al., 2006; Borg et al., 2008). In addition, the agglomeration of the nanoparticles made many of the active sites inaccessible. These were the main disadvantages of the treatment for the removal of sodium compounds, since it was not possible to maintain the size of the impregnated nanoparticles.

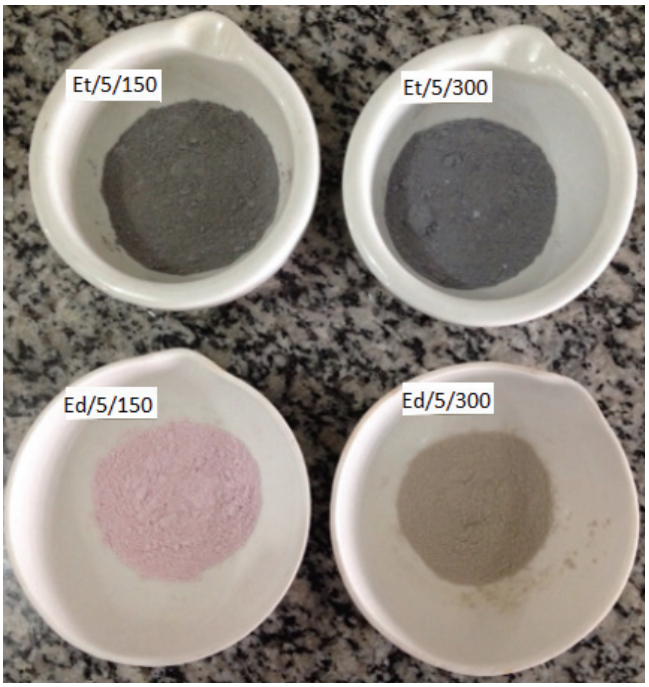

Figure 6. Co/SBA-15 catalysts after leaching and heat treatment.

Table 4. Catalytic Performance in the Fischer-Tropsch Synthesis.

Catalyst	Flow (mL min.$^{-1}$)	Reaction time hour^{-1}	X_{CO} (%)	Selectivity (%)				
				CH_4 (methane)	C_2–C_4 (light)	C_5–C_{12} (gasoline)	C_{12}–C_{18} (diesel)	C_{19}^+
Et/5/150	30	0,1	7	50.3	28.7	7.9	0.4	12.7
	30	24	10	53.7	31.4	7.9	0.3	6.7
Et/5/300	30	0.1	8	41.7	24.7	5.9	0.5	27.1
	30	24	9	51.0	28.6	6.8	0.4	13.2
Ed/5/150	30	0.1	8	53.7	30.6	9.7	0.5	5.4
	30	24	4	55.6	31.3	8.6	0.4	4.2
Ed/5/300	30	0.1	10	46.9	32.6	11.0	0.8	8.7
	30	24	6	54.5	31.0	8.1	0.3	6.0

Moreover, there was a greater formation of waxes in catalysts in which the temperature of heat treatment was higher, as had already been presented in the literature (Mochizuki et al., 2007). This behaviour probably occurred because of the larger particle size in the catalysts in which the treatment temperature was higher, because consequently there was a greater sintering of the nanoparticles present and increased pore blockage.

Another evidence of pore blockade is the decrease in gasoline and diesel selectivity after 24 hours of reaction, mainly in EDTA-treated catalysts, which presented higher particle sizes than ethanol-treated catalysts, as can be demonstrated in TEM analysis.

Therefore, the results showed that the Co/SBA-15 catalysts with nanoparticle sizes above 20 nm did not present significant differences of conversion and selectivity, mainly in relation to hydrocarbons in the gasoline and diesel range.

Conclusion

The results found in this study indicate the complexation power of EDTA is greater than the dissolution power of ethanol in the removal of sodium nitrate of Co/SBA-15 catalysts. In addition, the heat treatment step seems to potentiate the removal of unwanted compounds. However, although the treatment had removed most of the sodium compounds, there was much agglomeration of the cobalt nanoparticles. Accordingly, the efficacy in the removal of sodium compounds through leaching and heat treatment is annulled by the agglomeration of nanoparticles, making the catalysts unattractive when used in the FTS to obtain long chain hydrocarbons.

Acknowledgements

The authors are grateful to *Coordenação de Aperfeiçoamento de Pessoal de Nível Superior* (Capes/Brazil) and *Conselho Nacional de Desenvolvimento Científico e Tecnológico* (CNPq/Brazil) for financial support and to the *Complexo de Centrais de Apoio à Pesquisa* (Comcap/UEM) and the Brazilian Nanotechnology National Laboratory (LNNano/Brazil) for TEM and HRTEM analyses.

References

An, X., Wu, B., Hou, W., Wan, H., Tao, Z., Li, T., ... Yi, F. (2007). The negative effect of residual sodium on iron-based catalyst for Fischer–Tropsch synthesis. *Journal of Molecular Catalysis A: Chemical, 263*(1-2), 266-272. doi: 10.1016/j.molcata.2006.09.003

Balonek, C. M., Lillebø, A. H., Rane, S., Rytter, E., Schmidt, L. D., & Holmen, A. (2010). Effect of alkali metal impurities on Co-Re catalysts for Fischer-Tropsch Synthesis from biomass derived syngas. *Catalysis Letters, 138*(1-2), 8-13. doi: 10.1007/s10562-010-0366-4

Barrett, E. P., Joyner, L. G., & Halenda, P. P. (1951). The determination of pore volume and area distributions in porous substances. I. Computations from nitrogen isotherms. *Journal of the American Chemical Society, 73*(1), 373-383. doi: 10.1021/ja01145a126

Bezemer, G. L., Bitter, J. H., Kuipers, H. P. C. E., Oosterbeek, H., Holewijn, J. E., Xu, X., ... Jong, K. P. (2006). Size effects in the Fischer-Tropsch reaction studied with carbon nanofiber supported catalysts. *Journal of the American Chemical Society, 128*(12), 3956-3964. doi: 10.1021/ja058282w

Borg, Ø., Dietzel, P. D. C., Spjelkavik, A. I., Tveten, E. Z., Walmsley, J. C., Diplas, S., ... Rytter, E. (2008). Fischer-Tropsch synthesis: Cobalt particle size and support effects on intrinsic activity and product distribution. *Journal of Catalysis, 259*(2), 161-164. doi: 10.1016/j.jcat.2008.08.017

Borg, Ø., Hammer, N., Enger, B. C., Myrstad, R., Lindvåg, O. A., Eri, S., ... Rytter, E. (2011). Effect of biomass-derived synthesis gas impurity elements on cobalt Fischer-Tropsch catalysts performance including in situ sulphur and nitrogen addition. *Journal of Catalysis, 279*(1), 163-173. doi: 10.1016/j.jcat.2011.01.015

Brunauer, S., Emmett, P. H., & Teller, E. (1938). Adsorpion of gases in multimolecular layers. *Journal of the American Chemical Society, 60*(2), 309-319. doi: 10.1021/ja01269a023

Dalai, A. K., & Davis, B. H. (2008). Fischer-Tropsch synthesis: A review of water effects on the performances of unsupported and supported Co catalysts. *Applied Catalysis A: General, 348*(1), 1-15. doi: 10.1016/j.apcata.2008.06.021

Davis, B. H. (2003). Fischer-Tropsch synthesis: relationship between iron catalyst composition and process variables. *Catalysis Today, 84*(1-2), 83-98. doi: 10.1016/S0920-5861(03)00304-3

Dry, E. (1996). Practical and theoretical aspects of the catalytic Fischer-Tropsch process. *Applied Catalysis A: General, 138*(2), 319-344. doi: 10.1016/0926-860X(95)00306-1

Khodakov, A. Y., Chu, W., & Fongarland, P. (2007). Advances in the development of novel cobalt Fischer-Tropsch catalysts for synthesis of long-chain hydrocarbons and clean fuels. *Chemical Reviews, 107*(5), 1692-1744. doi: 10.1021/cr050972v

Kruk, M., & Jaroniec, M. (1997). Application of large pore MCM-41 molecular sieves to improve pore size analysis using nitrogen adsorption measurements. *Langmuir, 13*(23), 6267-6273. doi: 10.1021/la970776m

Lillebø, A. H., Patanou, E., Yang, J., Blekkan, E. A., & Holmen, A. (2013). The effect of alkali and alkaline earth elements on cobalt based Fischer-Tropsch catalysts. *Catalysis Today, 215*, 60-66. doi: 10.1016/j.cattod.2013.03.030

Loosdrecht, J., Haar, M., Kraan, A. M., Dillen, A. J., & Geus, J. W. (1997). Preparation and properties of supported cobalt catalysts for Fischer-Tropsch synthesis. *Applied Catalysis A: General, 150*(2), 365-376. doi: 10.1016/S0926-860X(96)00306-7

Martínez, A., López, F., Márquez, F., & Díaz, I. (2003). Fischer–Tropsch synthesis of hydrocarbons over mesopororous Co/SBA-15 catalysts: the influence of metal loading, cobalt precursor, and promoters. *Journal of Catalysis, 220*(2), 486-499. doi: 10.1016/S0021-9517(03)00289-6

Martínez, A., Prieto, G., & Rollan, J. (2009). Nanofibrous γ-Al_2O_3 as support for Co-based Fischer-Tropsch catalysts: Pondering the relevance of diffusional and dispersion effects on catalytic performance. *Journal of Catalysis, 263*(2), 292-305. doi: 10.1016/j.jcat.2009.02.021

Mochizuki, T., Hara, T., Koizumi, N., & Yamada, M. (2007). Surface structure and Fischer-Tropsch synthesis activity of highly active Co/SiO_2 catalysts prepared from the impregnanting solution modified with some chelating agents. *Applied Catalysis A: General, 317*, 97-104. doi: 10.1016/j.apcata.2006.10.005

O'Brien, R. J., Xu, L., Spicer, R. L., Bao, S., Milburn, D. R., & Davis, B. H. (1997). Activity and selectivity of precipitated iron Fischer-Tropsch catalysts. *Catalysis Today, 36*(3), 325-334. doi: 10.1016/S0920-5861(96)00246-5

Ramos, A. L. D., Marques, J. J., Santos, V., Freitas, L. S., Santos, R. G. V. M., & Souza, M. M. V. M. (2011). Atual estágio de desenvolvimento da tecnologia GTL e perspectivas para o Brasil. *Química Nova, 34*(10), 1704-1716. doi: 10.1590/S0100-40422011001000004

Schwarzenbach, G., & Flaschka, H. A. (1969). *Complexometric Titrations*. London, UK: Methuen Young Books.

Sun, S., & Murray, C. B. (1999). Synthesis of monodisperse cobalt nanocrystals and their assembly into magnetic superlattices (invited). *Journal of Applied Physics, 85*(8), 4325-4330. doi: 10.1063/1.370357

Tam, M. S., Gunter, G. C., Craciun, R., Miller, D. J., & Jackson, J. E. (1997). Reaction and spectroscopic studies of sodium salt catalysts for lactic acid conversion. *Industrial & Engineering Chemistry Research, 36*(9), 3505-3512. doi: 10.1021/ie970014m

Wang, Y., Wu, H., Zhang, Q., & Tang, Q. (2005). Cobalt nanoparticles prepared in Faujasite zeolites by borohydride reduction. *Microporous and Mesoporous Materials, 86*(1-3), 38-49. doi: 10.1016/j.micromeso.2005.07.001

Zhao, D., Feng, J., Huo, Q., Melosh, N., Fredrickson, G. H., Chmelka, B. F., & Stucky, G. D. (1998). Triblock copolymer syntheses of mesoporous silica with periodic 50 to 300 angstrom pores. *Science, 279*(5350), 548-552. doi: 10.1126/science.279.5350.548

Zhao, D., Sun, J., Li, Q., & Stucky, G. D. (2000). Morphological control of highly ordered mesoporous silica SBA-15. *Chemistry of Materials, 12*(2), 275-279. doi: 10.1021/cm9911363

Zhao, Y., Zheng, R. K., Zhang, X. X., & Xiao, J. Q. (2003) A simple method to prepare uniform Co nanoparticles. *IEEE Transactions on Magnetics, 39*(5), 2764-2766. doi: 10.1109/TMAG.2003.815592